J|A|C|S COMMUNICATIONS

Published on Web 01/02/2009

Hydrophilicity-Controlled Carbon Aerogels with High Mesoporosity

Yousheng Tao,*,† Morinobu Endo,† and Katsumi Kaneko‡

Institute of Carbon Science and Technology, Faculty of Engineering, Shinshu University, Nagano 380-8553, Japan, and Department of Chemistry, Chiba University, Chiba 263-8522, Japan

Received October 21, 2008; E-mail: tao@endomoribu.shinshu-u.ac.jp

Nanoporous carbons consisting of three-dimensional interconnected micropores and mesopores have many desirable properties that make such materials the focus of great interest.[1,2] These carbon materials have higher diffusion efficiency and a larger surface area than unimodal carbon materials and have been extensively used for various applications such as catalyst support, gas adsorption and separation, water purification, and battery electrodes.[3,4] Carbon aerogels, a representative nanoporous carbon, are a version of the organic polymer resorcinol−formaldehyde (RF) aerogels. They are pyrolyzed in an inert atmosphere such as nitrogen, while RF aerogels are synthesized by sol−gel polycondensation of resorcinol with formaldehyde followed by CO_2 supercritical drying.[5] They are expected to have a wide variety of applications such as hydrogen fuel storage, catalysis, electrical charge storage, and chromatographic separation.[6] Very recently, the use of carbon aerogels as a hard template for advanced materials has been suggested, and mesoporous zeolites have been synthesized using carbon aerogel templating.[7] Carbon aerogels with desirable nanostructures and surface properties are clearly needed for various applications.

In this Communication, we report a unique method of producing highly mesoporous carbon aerogels with hydrophilicity-controlled pore walls. It uses CO_2 supercritical drying to form interconnected micropores and small mesopores and, at the same time, uses colloidal silica nanocasting to form larger mesopores and increase pore volume. Controlled removal of the silica from the pore walls not only increases the nanoporosity but also modifies the hydrophilicity of the walls.

Product synthesis was carried out using sol−gel polymerization of resorcinol (R) and formaldehyde (F) with sodium carbonate (C) as a catalyst in the presence of colloidal silica particles (Ludox HS-40). The molar ratio of the starting mixture was 1 R:2 F:0.0025 C:2 SiO_2:5 H_2O. The gels were transformed into silica/RF aerogels by CO_2 supercritical drying and then transformed into silica/carbon aerogels by pyrolysis in a nitrogen atmosphere. Controlled partial silica removal or complete silica removal with aqueous HF solution resulted in a silica-modified carbon aerogel (SMCA) or a highly mesoporous carbon aerogel (HMCA), respectively. Thermogravimetric analysis indicated that the silica contents of the HMCA and SMCA were 0 and 22 wt. %. We also prepared, for comparison purpose, a carbon aerogel (CA) without silica and silica-templated mesoporous carbon (TMC) without CO_2 supercritical drying.

The N_2 adsorption isotherms of the products at 77 K are shown in Figure 1. The nitrogen adsorption isotherms were basically IUPAC type-IV isotherms. The adsorption below $P/P_0 = 0.1$ indicates the presence of micropores, and the adsorption at a higher relative pressure indicates the presence of mesopores. The explicit adsorption hysteresis loops for the SMCA and HMCA suggest that they were highly mesoporous. The mesopore size distributions

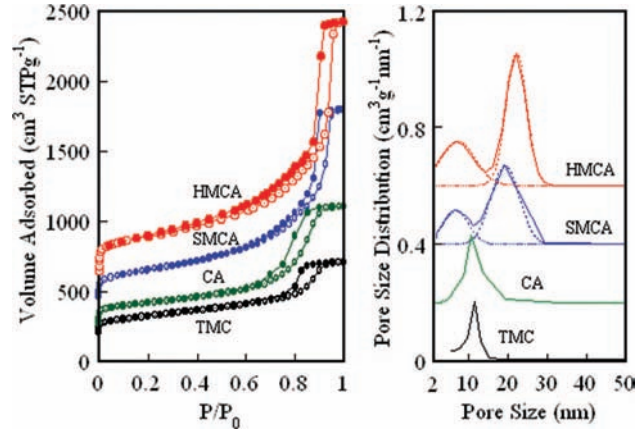

Figure 1. N_2 adsorption (○)/desorption (●) isotherms at 77 K for HMCA, SMCA, CA, and TMC (left) and BJH mesopore size distributions (solid line) and fitting curves of Gauss function (dotted lines) (right). Isotherms for CA, SMCA, and HMCA were vertically shifted 200, 400, and 600 cm^3 STP g^{-1}, respectively. Distributions of mesopore size for CA, SMCA, and HMCA were offset vertically by 0.2, 0.4, and 0.6 cm^3 g^{-1} nm^{-1}, respectively.

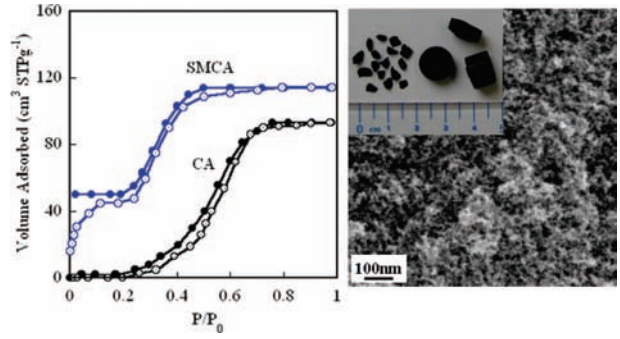

Figure 2. Water adsorption (○)/desorption (●) isotherms at 303 K for SMCA and CA (left) and FE-SEM image and photograph (inset) of SMCA (right).

Table 1. Pore Structural Parameters of the Products

	S_{BET} m^2 g^{-1}	micropore size (nm)	micropore vol (cm^3 g^{-1})	mesopore size (nm)	mesopore vol (cm^3 g^{-1})
HMCA	1500	0.65	0.64	6.5, 22.0	2.20
SMCA	1040	0.61	0.44	6.2, 18.5	1.73
CA	715	0.64	0.33	10.5	0.90
TMC	670	0.60	0.28	12.0	0.57

(MPSDs) derived from the desorption branches of the isotherms using the BJH (Barrett−Joyner−Halenda) method[8] indicate that the CA and TMC had relatively small mesopores with the MPSD centered at 10.5 and 12.0 nm, respectively. The MPSDs of the SMCA and HMCA were bimodal with peaks at 6.2 and 18.5 nm and 6.5 and 22.0 nm, respectively. The pore structural parameters

† Shinshu University.
‡ Chiba University.

10.1021/ja808132u CCC: $40.75

determined from the N_2 adsorption are summarized in Table 1. The results of the N_2 adsorption analysis suggest that micropores and small mesopores of the SMCA, HMCA, and CA resulted from the CO_2 supercritical drying while those of the TMC resulted from the silica templating. Silica templating can lead to the formation of larger mesopores in SMCAs and HMCAs. Ludox HS-40 silica has an average particle size of ~12 nm. Since it was used as a hard template, there should be pores with a size of ~12 nm in the resulting carbon materials. The fact that single silica particles are cast in carbonic walls with pores ~6 nm in size means that removal of the silica particles in part or whole was responsible for the formation of larger mesopores (18.5 or 22.0 nm) in the products. The individual silica particles acted as a hard template, which supports our synthesis strategy.

Since the micropores and small mesopores can be tuned through solution chemistry,[7] and since silica templates of different nanosizes are readily available, our proposed method can be used to prepare desirable nanostructured carbon aerogels. Moreover, since the pore systems are generated at different stages during the synthesis, controllable chemical functionalities of the pore walls can be achieved through independent modification of the pore systems. Next, we will show that controlled removal of the silica can modify the hydrophilicity of the products. The silica template is connected to already developed micropores and small mesopores among the carbonic skeletons, making the removal of the template by HF or NaOH etching much easier compared to a pure nanocasting process.

Water adsorption isotherms of SMCA at 303 K are shown in Figure 2, including that of CA for comparison. The CA and SMCA exhibited quite different water adsorption behaviors. The water adsorption isotherms of CA show adsorption uptake in the medium relative pressure region near $P/P_0 = 0.5$ without a clear adsorption hysteresis. The water adsorption isotherms of the SMCA show relative steep uptakes below $P/P_0 = 0.2$ and near $P/P_0 = 0.4$. The adsorption amounts for the SMCA and CA in the medium relative pressure regions are comparable and possibly associated with micropore filling of the water molecular clusters. The micropore sizes of these carbon materials are suitable for the unit sizes of water molecular clusters, giving rise to no marked hysteresis.[8] The water adsorption below $P/P_0 = 0.2$ can be associated with the hydrophilic property of the silica on the pore walls of the products, while the hysteresis on desorption below $P/P_0 = 0.2$ must be caused by the retained water, being indicative of the hydrophilic silica on the mesopore walls. The XPS spectra of the SMCA exhibited peaks at 103.8 eV (Si 2P), 533.1 eV (O 1s), and 284.1, 286.2 eV (C 1s), indicating carbon in multiple chemical states and the existence of silica at the surface (Figure 1S in Supporting Information). Si/C on the surface determined from XPS was 0.11, slightly higher than the bulk contents. The silica at the surface controlled the hydrophilicity of the pore walls. Hence, the characteristics of water adsorption on SMCA, which are different from those of either carbon or M41S materials, suggest that SMCAs have both hydrophobic and hydrophilic pore walls.

The products can be obtained in monolith or powder form (Figure 2). The field-emission scanning electron micrograph (FE-SEM) image of an SMCA clearly shows randomly distributed mesopores and significant mesoporosity (Figure 2S in Supporting Information).

The short-range microstructures of SMCAs, HMCAs, and CAs were probed using the Raman effect. In the Raman spectrum of each sample (Figure 3S in Supporting Information), two distinct peaks were observed at shifts of 1360 and 1580 cm^{-1} and are respectively assigned to disordered (D band) and ordered (G band) graphitic carbons. The ratio of the integrated intensity of the G band to that of the D band was independent of the presence of silica and nanopores, indicating that the graphene ribbons in the products had the same in-plane structural order as a carbon aerogel.

Carbon-based xerogels were previously shown to have excellent electrochemical performance due to their high electrical conductivity, large nanoporosity, and three-dimensional pore connectivity.[9] Similarly, silica-modified carbon aerogels can have better electrochemical performance because a better solid electrolyte interface (a passivation layer) film can be formed on the silica-modified carbon surface.[10] We will present a detailed discussion of the results of electrochemical studies on such materials in a forthcoming paper.

In summary, we prepared highly mesoporous carbon aerogels with hydrophilicity-controlled pore walls using an approach that combines CO_2 supercritical drying and colloidal silica nanocasting. Owing to their high surface area and large nanopore volume, as well as the hydrophilicity-controlled pore walls, these materials can be used as adsorbents, anodes for lithium ion batteries, electrochemical supercapacitors, and potential supports for heterogeneous catalysis of bulkier molecules for which the diffusion of reactant molecules could be facilitated.

Acknowledgment. This research was supported by CLUSTER (the second stage) of Ministry of Education, Culture, Sports, Science and Technology, Japan, and by a project (no. 18-06059) from Japan Society for the Promotion of Science (JSPS).

Supporting Information Available: Synthesis recipe, characterization methods, and figures with FE-SEM images, Raman and XPS spectra. This material is available free of charge via the Internet at http://pubs.acs.org.

References

(1) (a) Marsh, H.; Rodrı´guez-Rrinoso, F. *Activated Carbon*; Elsevier: Oxford, 2006; pp 383−447. (b) Bottani, E. J.; Tascón, J. M. D. *Adsorption by Carbons*; Elsevier: Oxford, 2006; pp 565−590.
(2) (a) Kyotani, T. *Carbon* **2000**, *38*, 269–286. (b) Rodrı´guez-Rrinoso, F. In *Introduction to Carbon Technology*; Marsh, H., Heintz, E. A., Rodrı´guez-Rrinoso, F., Eds.; Universidad de Alicante: Alicante, Spain, 1997; pp 35.
(3) (a) Baker, F. S.; Miller, C. M.; Repik, A. J.; Tolles, E. D. In *Kirk-Othmer Encyclopedia of Chemical Technology*; Howe-Grant, M., Ed.; John Wiley: New York, 1992; Vol. 4, pp 1015−1037. (b) Rodrı´guez-Rrinoso, F. In *Handbook of Porous Solids*; Schüth, F., Sing, K. S. W., Weitkamp, J., Eds.; Wiley-VCH: Weinheim, Germany, 2002; pp 1766−1827.
(4) (a) Joo, S. H.; Choi, S. J.; Oh, I.; Kwak, J.; Liu, Z.; Terasaki, O.; Ryoo, R. *Nature* **2001**, *412*, 169–172. (b) Al-Muhtaseb, S. A.; Ritter, J. A. *Adv. Mater.* **2003**, *15*, 101–114.
(5) Pekala, R. W. *J. Mater. Sci.* **1989**, *24*, 3221–3227.
(6) (a) Lu, X.; Arduini-Schuster, M. C.; Kuhn, J.; Nilsson, O.; Frick, J.; Pekala, R. W. *Science* **1992**, *255*, 971–972. (b) Pekala, R. W.; Coronado, P. R.; Calef, D. F. *Carbon Aerogels for Hydrogen Storage*; US DOE Report; U.S. Department of Energy: Washington, DC, 1994; p 227. (c) Moreno-Castilla, C.; Maldonado-Hódar, F. J. *Carbon* **2005**, *43*, 455–465.
(7) (a) Tao, Y.; Kanoh, H.; Kaneko, K. *J. Am. Chem. Soc.* **2003**, *125*, 6044–6045. (b) Tao, Y.; Kanoh, H.; Abrams, L.; Kaneko, K. *Chem. Rev.* **2006**, *106*, 896–910.
(8) (a) Barrett, E. P.; Joyner, L. G.; Halenda, P. P. *J. Am. Chem. Soc.* **1951**, *73*, 373–380. (b) Ohba, T.; Kanoh, H.; Kaneko, K. *J. Am. Chem. Soc.* **2004**, *126*, 1560–1562.
(9) Tao, Y.; Endo, M.; Ohsawa, R.; Kanoh, H.; Kaneko, K. *Appl. Phys. Lett.* **2008**, *93*, 193112.
(10) Wang, Y. X.; Nakamura, S.; Ue, M.; Balbuena, P. B. *J. Am. Chem. Soc.* **2001**, *123*, 11708–11718.

JA808132U